journal

Co-sintering Zirconia Electrolyte and Insulator Tapes for Sensor Applications

Wenxia Li,*,† Alvin Feingold,* Ponnusamy Palanisamy,* and Gerald Lorenz*

ESL ElectroScience Inc., 416 East Church Rd, King of Prussia, Pennsylvania 19406

Multilayer co-sintered ceramics (HTCC or LTCC) are widely used for planar sensors (such as gas sensors for oxygen, hydrogen, hydrocarbon, carbon monoxide, as well as, NOx, etc.) as well as solid oxide fuel cells, and other special applications such as high-temperature batteries and transformers for deep-well drilling. Ceramic tapes with different sintering behaviors can be modified so they can be co-sintered to build multilayer devices. One of the main challenges in building these devices is the co-sintering of a dissimilar material structure. In this study, co-sintering of yttria stabilized zirconia and insulator tapes was studied. Their sintering behaviors were modified so that the effects of sintering shrinkage and sintering rate could be separated from coefficient of thermal expansion (CTE) effects. It was found that "co-burnout" has a strong effect on the delamination and cracking of the multilayer structures built with these dissimilar materials. The layer configuration in the co-sintering structure also plays a strong role in determining the tolerance for sintering (sintering shrinkage and sintering rate) mismatch. The CTE and the sintering behavior of insulator tapes were modified to match those of zirconia tapes. Co-sintering behavior of the modified insulator and zirconia tapes was examined. The effect of sintering mismatch on camber in multilayer structures is also discussed.

I. Introduction

IN many multilayer high-temperature co-fired ceramic (HTCC) parts, a heater circuit is buried in between zirconia layers together with the functional circuit. To minimize the heater interference on the functional circuit, an insulator is used to isolate the heater electrically from the functional circuit. The insulator is typically an alumina-based material. Co-sintering alumina and zirconia together has been a challenge for decades[1,2] for the following reasons:

1. Alumina sinters less readily than zirconia at the same particle size/surface area at typical sintering temperatures due to the inherent nature of these materials; this results in significantly different sintering rates.
2. The coefficient of thermal expansion (CTE) of alumina and zirconia are significantly different: $6–8 \times 10^{-6}$ K^{-1} for alumina versus $9–11 \times 10^{-6}$ K^{-1} for zirconia.

Although in an actual HTCC part such as a planar oxygen sensor element, complex features such as inner and outer electrodes and air channel are built into the multilayer configuration, the dominant factor for minimizing camber and defects in the parts is the co-sintering of the zirconia and insulator layers. In other words, it needs to be demonstrated that a simple multilayer structure consisting of zirconia and insulator layers can be sintered flat and delamination free

before one can succeed in co-sintering complex functional parts with embedded features such as electrode, channel, and heater.

In previous studies[1–7] on co-sintering of alumina and zirconia, effects of thickness and layer structure on crack formation were reported. Typically, cracks resulting from sintering mismatch have wider openings and rounded crack edges. Cracks due to mismatch of CTE have fine openings and sharp crack edges.[1] However, none of the research separated the effects of sintering mismatch from those of CTE mismatch. Green *et al.*[8] summarized all aspects that fall into constrained sintering. It is well agreed[2–8] that the faster shrinking layer will be in equibiaxial tension whereas the slower shrinking layer will be in equibiaxial compression.

Ravi and Green[9] studied the co-sintering of a bilayer structure by adjusting the green density of the same powder in tape casting. It is found that the bilayer structure bent toward the faster shrinking layer. However, no sandwich structure was tested in the study. Sun *et al.*[10] investigated powder selection to match the sintering rate of zirconia and alumina. Once the sintering rate matched between the different materials, no significant dimensional mismatch could occur at any time during sintering, thus reducing the possibility for cracks and camber in the sample. Although a crack- and camber-free functionally graded material was produced under a certain firing condition, CTE mismatch is still in the system. The effect of CTE mismatch was not discussed in the study.

Co-sintering is also widely used in planar SOFC research and manufacturing. Lee *et al.*[11] discussed how to apply constraint to co-sinter flat and crack-free LaSrMnO₃/YSZ/NiO-YSZ multilayer parts. LSM and YSZ bilayer was sintered at various temperatures; as expected, the bilayer part bent toward the faster shrinking layer.

In this study, zirconia tapes were used as the starting material to study sintering mismatch. A sandwich structure using two different zirconia tapes was prepared. By modifying the organic system used in the tapes, the sintering behavior of the zirconia tape can be modified without affecting the CTE. Thus, the sintering mismatch can be studied independent of CTE mismatch by using tapes made of the same ceramic powder but with different sintering behavior. By modifying insulator tapes to have a matched sintering behavior but a different CTE from zirconia, the CTE effects on the co-sintering stresses and camber can be examined independent of sintering mismatch. Then, both the sintering behavior and CTE of insulator tapes could be modified to match the zirconia tapes. The initial phase of this work focused on the sintering mismatch using zirconia tapes of two different green densities. Next we studied co-sintering of zirconia and insulator tape compositions. This study reports on the effects of sintering mismatch, CTE mismatch, and organic burnout on defects in the co-sintered multilayer structures.

II. Experimental Procedure

(1) Raw Materials
A 5 mol% YSZ (SSA: ~40 m^2/cm^3, commercially available) powder was used for the zirconia tape. Two organic systems

(Organic-A and Organic-B, both PVB-based solvent solutions) were used in these zirconia tapes (Z1-A and Z1-B). A tape (Z2-A) made of a 3 mol% YSZ (SSA: ~40 m^2/cm^3, commercially available) and Organic-A was also examined with Z1-B tape. The CTE of the 3 mol% YSZ is close to that of the 5 mol% YSZ, but they have different sintering behaviors.

An alumina compound (SSA: ~50 m^2/cm^3; Atlantic Equipment, Bergenfield, NJ), sintering aids (silicate glass, T_s: 700°C–1300°C; Viox Corporation, Seattle, WA) and CTE adjusters (an oxide ceramic powder: SSA: ~18–25 m^2/cm^3, CTE: ~14 × 10^{-6} K^{-1}, JT Baker, Phillipsburg, NJ) were used to make the insulator tapes. Two insulator tapes labeled as I-1 and I-2 were cast to match Z1-A and Z1-B, respectively. As these did not match the zirconia tapes as well as expected, the zirconia tapes were modified to try to match the insulator tapes. MZ1 & MZ2 were formulated with 5 mol% YSZ powders with different surface areas from the original tapes. Organic-B was used to formulate these tapes. These tapes are summarized in Table I. The green oxide only density (GOOD) of the tape[12] as percentage of the calculated theoretical density of the ceramics is listed in the table as well.

(2) Sample Preparation

A 12-layer configuration was used for the co-sintering test (CST) parts. The following layer configuration was chosen to simulate the typical commercial planar oxygen sensor element structure. Top: layers 10–12, one zirconia tape. Middle: layers 8–9, another zirconia tape or insulator tape. Bottom: layers 1–7, same tape as layers 10–12.

The layups were laminated at 80°C and 2000 psi (14MPa) for 20 min. Then the laminates were cut into ~5 × 50 mm CST bar specimens. The CST bars (three to five pieces) were then fired at ≤ 1°C/min to 800°C, then ramped up at 1°C–5°C/min to 1450°C, where they were held for 1.5 h. Some specimens were fired at a lower temperature, 800°C or 1350°C, to examine the burnout and sintering temperature effects. The layer structure for the CST bar specimens is summarized in Table II.

(3) Sample Testing

A dilatometer (DIL 402C; Netzsch, Burlington, MA) was used to characterize both the sintering behavior and CTE for each tape. The dilatometer samples were made from 16 layers of zirconia tape or 32 layers of insulator tape, which were

laminated to a target green thickness of 2 mm. The laminates were then cut into short bars (~5 mm × 6.5 mm) and long bars (~5 mm × 19 mm) with parallel ends to facilitate mounting in the dilatometer. The short bars were run in the dilatometer at 5°C/min to 1550°C to obtain sintering curves. The long bars were fired with the CST specimens at 1450°C for 1.5 h. CTE was then measured using the fired long bars at 10°C/min to 1000°C in the dilatometer. In both cases, the bars were mounted horizontally with the probe sensing change in length.

After firing, the CST parts were examined visually for major cracks/delamination and under an optical microscope for smaller scale defects. The parts were then broken by hand to estimate the residual stresses. When large residual stresses are stored in the bars, and if the boundary between the dissimilar layers is weak, upon breaking, the layers will separate or become stepped along the boundary between the insulator and the zirconia.

The linear shrinkage was measured on a four-hole sample. Four layers of zirconia tape or eight layers of insulator tape were laminated, and then cut into approximately 2 × 2 inch (50 × 50 mm) squares. Four holes of Φ0.25″ (Φ6.35 mm) were punched in an approximately 1 inch (25 mm) square pattern. The distance between the holes was measured before (Lo) and after sintering (Ls) at 1450°C for 1.5 h. The shrinkage was calculated using the following equation:

$$\text{Shrinkage} = (\text{Lo-Ls})/\text{Lo} * 100.$$

Four distances were measured for each four-hole sample. For each tape, two four-hole samples were tested. The average of the eight shrinkage measurements for each tape was calculated. The fired four-hole samples were also used to measure the density by Archimedes method.

III. Experimental Results

(1) Sintering Curves for the Zirconia Tapes and the Insulator Tapes

The sintering curves (shrinkage versus temperature) of the zirconia tapes: Z1-A, Z1-B, and Z2-A are plotted in Fig. 1. Although Z1-A and Z1-B are made of same zirconia powder, they have significantly different sintering behaviors. However, their sintering curves seem to meet at the end of the sintering (Fig. 1). Z2-A and Z1-B showed similar sintering behavior under 1100°C, but start to divert above 1125°C. This deviation is maintained until the end of the sintering.

The sintering curve of the insulator tapes is plotted in Figs. 2(a) and (b). For comparison, the sintering curve for the modified zirconia tapes is shown in these figures as
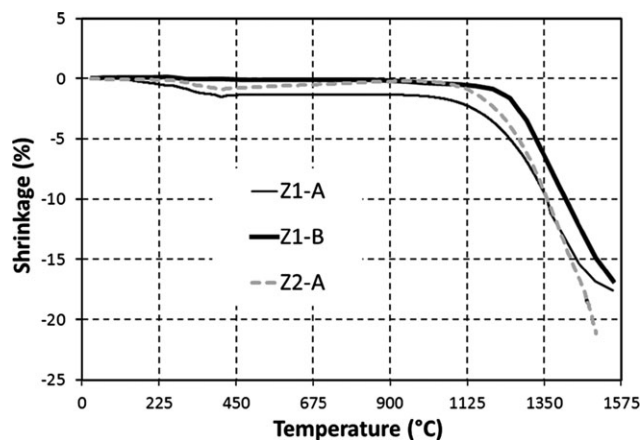
Table I. Summary of Tapes Cast

Tape	Description	GOOD, % of theoretical density
Z1-A	5 mol% zirconia, organic-A	51
Z1-B	5 mol% zirconia, organic-B	53
Z2-A	3 mol% zirconia, organic-A	47
I-1	Insulator composition to match Z1-A	46
I-2	Insulator composition to match Z1-B	48
MZ1	5 mol% zirconia, SSA 1, organic-B	49
MZ2	5 mol% zirconia, SSA 2, organic-B	45

All the zirconia tapes were cast at ~125 μm thickness. All the insulator tapes were cast at ~65 μm thickness. GOOD, green oxide only density.

Table II. Summary of CST Bars

Specimen	A1	A2	B1	B2	C	D
Layers 10–12	Z1-A	Z1-B	Z2-A	Z1-B	MZ1	MZ2
Layers 8–9	Z1-B	Z1-A	Z1-B	Z2-A	I-1	I-2
Layers 1–7	Z1-A	Z1-B	Z2-A	Z1-B	MZ1	MZ2

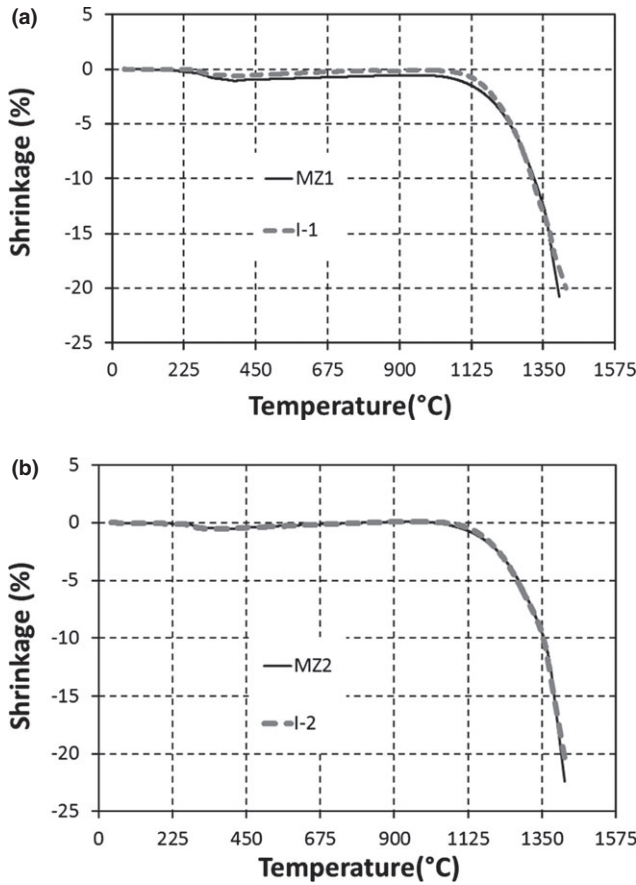**Fig. 1.** Sintering curves for Z1-A, Z1-B, and Z2-A tapes.

(a)

(b)

Fig. 2. Sintering curves of the insulator tapes; the sintering curves of the modified zirconia tapes are shown for comparison. (a) I-1 and MZ1; (b) I-2 and MZ2.

(a)

(b)

Fig. 3. Sintering rate versus temperature for I-2 and MZ2 tapes (a) from room temperature to 1400°C; (b) zoom in of (a) in the temperature range 1150°C–1400°C.

well. The MZ1 and I-1 show similar sintering behavior under 1350°C with only a small deviation in the range 675°C–1200°C. Above 1350°C, the sintering curves start to divert from each other. The MZ2 and I-2 almost overlap in their sintering behavior below 1350°C. Again, the sintering curves start to divert from each other above 1350°C. This is more obvious when observing the sintering rate (shrinkage change over temperature change) in Fig. 3.

The sintering rate of the Z1-A, Z1-B, and Z2-A is plotted in Figs. 4(a) and (b). No significant difference was observed below 1100°C among these tapes. Slight sintering rate differences are observed at 1100°C–1200°C and above 1350°C [Fig. 4(b)].

The sintering rate of the insulator tapes is shown in Figs. 3(a) and (b) and 5(a) and (b). For comparison, the sintering rate of the modified zirconia tapes is shown in Figs. 3 and 5 as well. No significant mismatch was observed below 1350°C between either I-1 and MZ1 or I-2 and MZ2. Above 1350°C, the sintering rate difference becomes significant. By comparing Figs. 3–5 it can be seen that the sintering rate difference among the zirconia tapes Z1-A, Z1-B, and Z2-A is much smaller than that between either I-1 and MZ1 or I-2 and MZ2. At 1400°C, about 0.03% °C^{-1} was observed among Z1-A, Z1-B, and Z2-A, whereas about 0.1% °C^{-1} for I-1 and MZ1, about 0.14% °C^{-1} for I-2 and MZ2.

(2) Sintered Properties for the Tapes

The linear shrinkage and relative density of each tape sintered at 1450°C for 1.5 h are shown in Table III. The CTE value for each fired tape is listed in Table III as well.
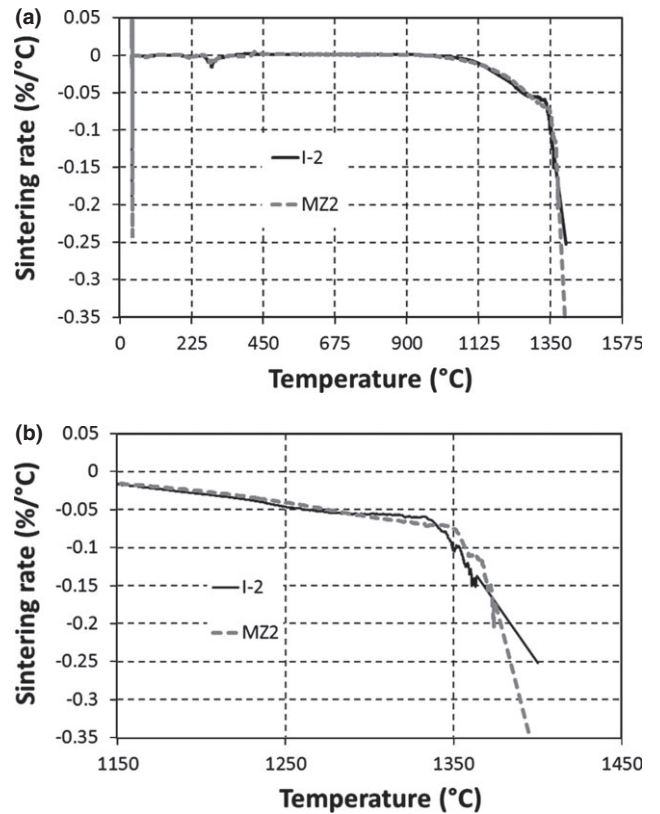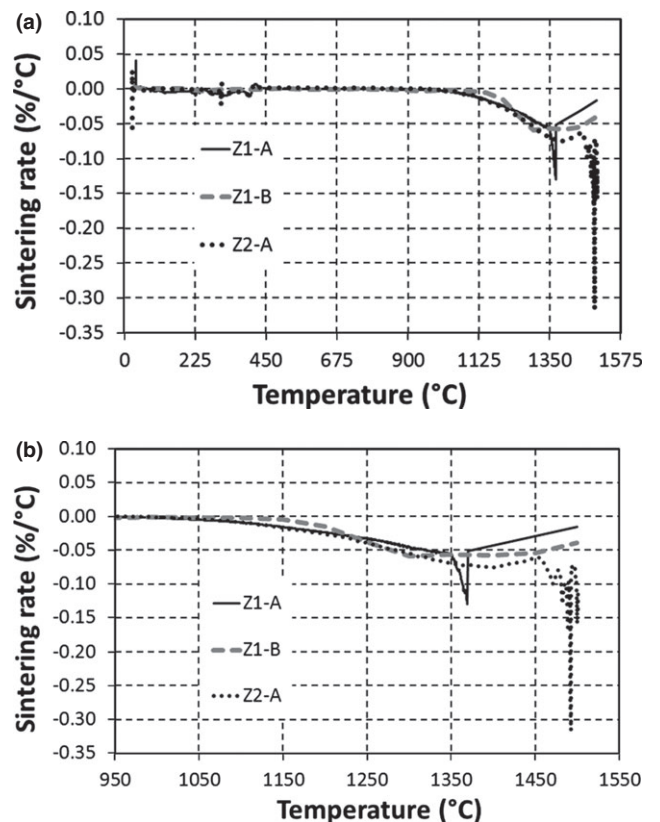

(a)

(b)

Fig. 4. Sintering rate versus sintering temperature for Z1-A, Z1-B, and Z2-A tapes (a) from room temperature to 1500°C; (b) zoom in of (a) in the temperature range 950°C–1500°C.
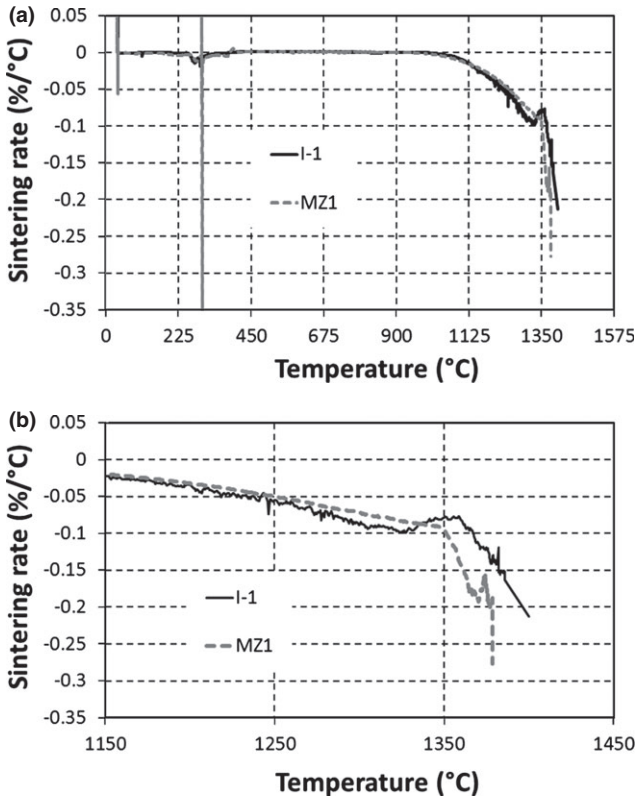
Fig. 5. Sintering rate versus temperature for I-1 and MZ1 tapes (a) from room temperature to 1400°C; (b) zoom in of (a) in the temperature range 1150°C–1400°C.

Table III. Sintered Tape Properties

	Shrinkage, %	Density, %	CTE, 10^{-6} K^{-1}
Z1-A	18.7	97.5	11.0
Z1-B	17.7	97.1	11.1
Z2-A	22.6	98.0	11.6
MZ1	22.8	98.4	11.3
MZ2	22.5	97.5	11.3
I-1	21.1	96.7	10.8
I-2	20.4	96.2	10.5

The differences in coefficient of thermal expansion (CTE) of the zirconia tapes are within experimental accuracy. The CTE of insulator tapes and the modified zirconia tapes appears to be matched fairly well; less than 7% difference is observed. The final shrinkage of the tapes varies some. The greatest difference (5.1%) is between Z1-B and MZ1.

(3) Visual Inspection and Hand Breaking of Co-sintered Samples

Table IV summarizes the results of visual inspection after the CSTs were sintered at various temperatures. The pictures of these parts are shown in Figs. 6 and 7.

IV. Discussion

In this study, as the CTE of the fired tapes is close to each other (Table III), only sintering mismatch is discussed.

(1) Co-burnout in Co-sintered Structures

As shown in Fig. 6, the specimen A1 delaminated in the corner around Z1-B layers after firing at 1450°C. This can be explained by the sintering behavior difference shown in Fig. 1. Z1-A shrinks earlier than Z1-B and causes separation. It is also noticed that even before the sintering begins, some delamination has occurred in the bar specimen, as seen in Table IV. The sintering behavior below 800°C is typically ignored because any associated dimensional change is small. However, in a multimaterial tape system, the tape burnout difference can cause defects. The dimensional change is critical, especially in the temperature range 450°C–800°C. In this temperature range, the organic binder burns out leaving a weakened part. Any movement, caused by dimensional change difference in the tapes due to the organics burnout difference, may generate stresses strong enough to cause cracking and delamination/separation between the layers. Similar behavior was observed with B1 sample, as shown in Fig. 6.

(2) Layer Configuration Effects on Co-sintering Stresses and Delamination

When layers are rearranged, different results are observed for A2 (compared with A1) and B2 (compared with B1), as shown in Fig. 6. A2 and A1 as well as B2 and B1 are made of same pairs of tapes except the relative position of the tapes in the laminate. A1 and B1 delaminated, whereas A2 and B2 did not. This can be explained by the sintering mismatch stresses generated by the different tape materials. Z1-A tape shrinks more than Z1-B tape. When the two tapes are put together, they tend to bend toward Z1-A.[8,11] In the CST bars, when the Z1-B is in layers 8 and 9 of the part, both the top and bottom Z1-A portions want to bend away from Z1-B. This shrinkage difference generates localized tensile stresses around Z1-B,[1,2] which pulls the Z1-A away from Z1-B. In A2, because Z1-A is in the layers 8 and 9 of the part, both the top and bottom portion of Z1-B want to bend toward Z1-A. In this configuration the sintering shrinkage difference generates localized compressive stresses around Z1-A.[1,2] This helps to hold the Z1-B in contact with the Z1-A. Similar mechanism holds for the B1 and B2 specimens. By controlling the layer configuration, some sintering mismatch can be tolerated as shown in Fig. 6 and Table IV.

Table IV. Visual Inspection and Hand-breaking Test on CST Bars

Specimens	Post 800°C, 0 min			Post 1350°C, 10 min			Post 1450°C, 1.5 h		
	Camber	Delam	Break	Camber	Delam	Break	Camber	Delam	Break
A1	0	1	n/a	−1	3	5	+1	4	5
A2	0	0	0	+1	0	0	0	0	0
B1	0	1	n/a	−2	4	5	−1	4	5
B2	0	0	0	0	0	0	0	0	0
C	−0.5	0.5	n/a	−2	1	4	−5	3	5
D	0	0	0	0	0	0	−4.5	0	0

Camber: 0, flat; 5, very curled; -, curled down; +, curled up.
Delam: 0, no delamination/separation; 5, fully delaminated.
Break: 0, no step when hand broken; 5, fully separated between the insulator and the zirconia layer.
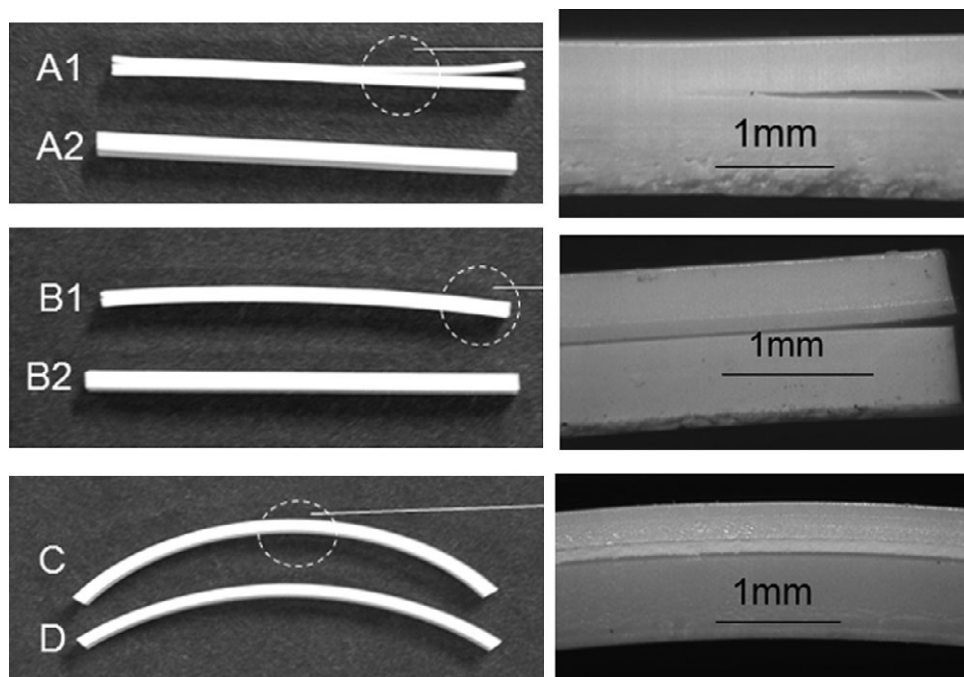
Fig. 6. Pictures taken from the side of the bar parts A1, A2, B1, B2, C, and D after firing at 1450°C for 1.5 h. The images on the right side are zoom in of the circled areas in the left.
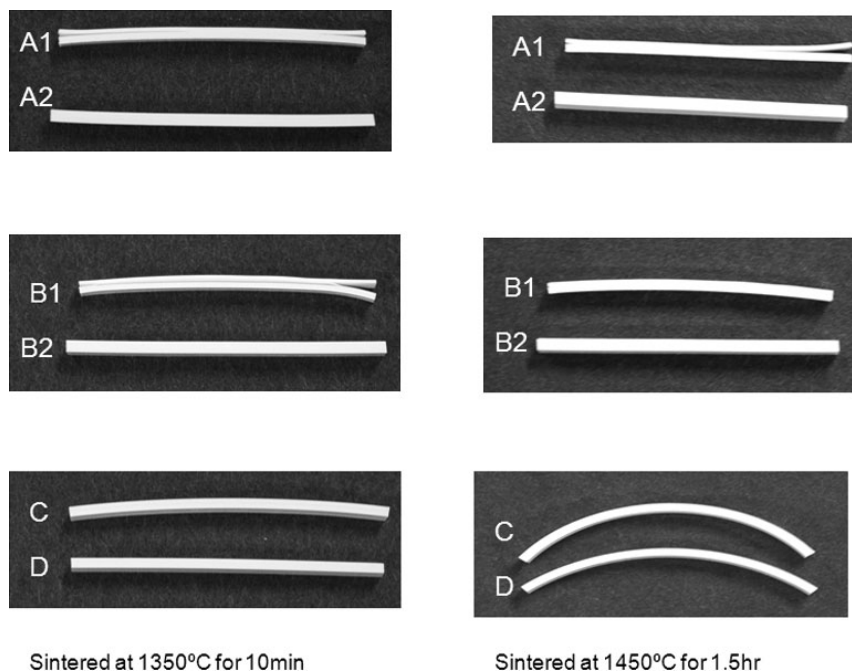

Sintered at 1350°C for 10min   Sintered at 1450°C for 1.5hr

Fig. 7. Pictures taken from the side of the bar parts A1, A2, B1, B2, C, and D sintered at 1350°C. For comparison, the pictures taken from the parts sintered at 1450°C are shown in the right column.

(3)   Camber and Co-sintering Mismatch

Because the CTE of the fired insulator tapes and the zirconia tapes is close to each other (Table III), the camber of the CST parts appear to be correlated with the sintering mismatch only. For samples C and D, when sintered at 1350°C, the parts came out relatively flat (shown in Fig. 7) due to the fact that the sintering curves almost overlap each other as shown in Figs. 2, 3(a) and (b), and 5. When sintered at 1450°C, the zirconia tape appears to shrink more and faster than the insulator tape, as indicated by the dilatometry shown in Figs. 3(b) and 5(b); note the separation of the curves above 1375°C. The parts fired at 1450°C are cambered much more than those fired at 1350°C, even though the final shrinkages of the insulator tapes are greater than those of the zirconia tapes. This suggests that the camber is more of a result of mismatched sintering rate rather than mismatched total sintering shrinkage.

Similar mechanism applies to samples A1, A2 and B1, B2. When fired at 1350°C or 1450°C, A1 curled down while A2 curled up a little bit. This is due to the fact that Z1-A shrinks faster and more than Z1-B during entire sintering. Therefore the part bends toward Z1-A, which is dominant. For A1, Z1-A is the bottom while it is close to the top for A2. That is why A1 curled down while A2 curled up. For B1

and B2, as Z2-A shrinks more and faster above 1125°C than Z1-B, B1 bent down regardless of whether it is fired at 1350°C or 1450°C. B2 remains almost flat whether fired at 1350°C or 1450°C. This may be due to the fact that the sintering rates for Z1-B and Z2-A between 1200°C and 1450°C are close to each other as shown in Fig. 4(b). Again, the camber seems to depend more on the sintering rate difference than the difference in total shrinkage.

Overall, A1, A2, B1, and B2 are much flatter than C and D when fired at 1450°C. This is consistent with the sintering rate mismatch as shown in Figs. 3(b), 4(b), and 5(b); the sintering rate mismatch in C and D ($>0.1\%$ °C^{-1} and $>0.14\%$ °C^{-1}, respectively) are much greater than that in A1, A2, B1, and B2 ($<0.03\%$ °C^{-1}) in the firing temperature range of 1350°C–1450°C.

V. Conclusions

1. Using CTE adjuster and sintering aids together with powder selection, the insulator tape can be modified to co-sinter with the zirconia tape to build multilayer devices.
2. Sintering mismatch can be accommodated by carefully selecting the layer configuration of a multilayer system. The faster shrinking layer in the middle of the structure resulted in a flat and delamination-free part.
3. Burnout rate is critical in multimaterial tape systems to prevent delamination before sintering occurs. Although the mismatch in burnout is very small compared with the sintering mismatch, it is strong enough to cause delamination/cracking in the system due to the fact that the system is weak, especially toward the end of burnout.
4. Camber from co-sintering depends more on the sintering rate mismatch than final sintering shrinkage difference. Even with final shrinkage difference of 4.9%, the part B2 fired flat and delamination free due to the similar sintering rate for the tapes Z1-B and Z2-A used to build B2 parts.

References

[1]P. Z. Cai, D. J. Green, and G. L. Messing, "Constrained Densification of Alumina/Zirconia Hybrid Laminates I: Experimental Observations of Processing Defects," *J. Am. Ceram. Soc.*, **80** [8] 1929–39 (1997).
[2]H. Schmid, O. Sbaizero, and S. Meriani, "Microstructure of Layered Zirconia/Alumina Composites"; pp. 665–70 in *Third Euro-Ceramics*, Vol. 3, Edited by P. Dura'n and J. F. Ferna'ndez. Faenza Editrice Iberica, Madrid, Spain, 1993.
[3]D. J. Green, P. Z. Cai, and G. L. Messing, "Residual Stresses in Alumina–Zirconia Laminates," *J. Eur. Ceram. Soc.*, **19** [13–14] 2511–7 (1999).
[4]H. Tomaszewskia, J. Strzeszewskib, and W. G bicki, "The Role of Residual Stresses in Layered Composites of Y–ZrO$_2$ and Al$_2$O$_3$," *J. Eur. Ceram. Soc.*, **19** [2] 255–62 (1999).
[5]O. Sbaizero and E. Lucchini, "Influence of Residual Stresses on the Mechanical Properties of a Layered Ceramic Composite," *J. Eur. Ceram. Soc.*, **16** [8] 813–8 (1996).
[6]P. Z. Caia, D. J. Green, and G. L. Messing, "Mechanical Characterization of Al$_2$O$_3$/ZrO$_2$ Hybrid Laminates," *J. Eur. Ceram. Soc.*, **18** [14] 2025–34 (1998).
[7]X. Wang and P. Xiao, "Residual Stresses and Constrained Sintering of YSZ/Al$_2$O$_3$ Composite Coatings," *Acta Mater.*, **52** [9] 2591–603 (2004).
[8]D. J. Green, O. Guillon, and J. Rödel, "Constrained Sintering: A Delicate Balance of Scales," *J. Eur. Ceram. Soc.*, **28**, 1451–66 (2008).
[9]D. Ravi and D. J. Green, "Sintering Stresses and Distortion Produced by Density Differences in Bi-layer Structures," *J. Eur. Ceram. Soc.*, **26**, 17–25 (2006).
[10]L. Sun, A. Sneller, and P. Kwon, "Powder Selection in Cosintering Multi-layered Ceramic Functionally Graded Materials Based on the Densification Kinetics Curves," *J. Compos. Mater.*, **43** [05] 469–82 (2009).
[11]S.-H. Lee, G. L. Messing, and M. Awano, "Sintering Arches for Cosintering Camber-Free SOFC Multilayers," *J. Am. Ceram. Soc.*, **91** [2] 421–7 (2008).
[12]R. E. Mistler and E. R. Twiname, *Tape Casting: Theory and Practice*. The American Ceramic Society, Westerville, OH, 173, 194, 2000. □